

Microbially driven fate of terrigenous particulate organic matter in oceans

Lianbao Zhang,¹ Mingming Chen,¹ Yue Zheng,² Jianning Wang,¹ Xilin Xiao,^{1,2} Xiaowei Chen,¹ Chen Hu,^{1,2} Jiaming Shen,¹ Jihua Liu,³ Kai Tang,¹ Dapeng Xu,¹ Qiang Shi,⁴ Xiaoyan Ning,⁵ Helmuth Thomas,^{4,6} Wei Qin,⁷ Meixun Zhao,⁵ Nianzhi Jiao,^{1*} Yao Zhang,^{1*}

¹State Key Laboratory of Marine Environmental Science and College of Ocean and Earth Sciences, Xiamen University, Xiamen, China

²College of the Environment and Ecology, Xiamen University, Xiamen, China

³Institute of Marine Science and Technology, Shandong University, Qingdao, China

⁴Department of Oceanography, Dalhousie University, Halifax, Nova Scotia, Canada

⁵Frontiers Science Center for Deep Ocean Multispheres and Earth System, Key Laboratory of Marine Chemistry Theory and Technology, Ministry of Education, Ocean University of China, Qingdao, China

⁶Institute of Carbon Cycles, Helmholtz Center Hereon, Geesthacht, Germany

⁷Department of Microbiology and Plant Biology, University of Oklahoma, Norman, Oklahoma

Abstract

A long-standing enigma in oceanography is why terrestrial organic matter is “missing” in the global ocean, despite the considerable discharge into it every year. Although some explanations, such as mineralogical composition, hydrodynamic processes, and priming effect, have been proposed, we hypothesize that the essential mechanism behind the missing organic matter is microbial processing, for which the underlying coupled geochemical, molecular, and genetic evidence is unknown. An ultra-large-volume, long-term river–seawater stratified simulation system was constructed to unravel the microbially driven fate of terrigenous particulate organic matter (POM) in oceans. Analysis of combining the molecular with POM chemical composition data suggests that Bacteroidetes could act as pioneers in the processing of terrigenous POM in oceans, degrading high-molecular-weight, high-carbon compounds such as polysaccharides. Remaining low-molecular-weight nitrogenous organic matter is subsequently degraded by Planctomycetes and Proteobacteria. Isotopic signals show that this preferential degradation causes a distinct “aging” effect of POM, and along with nitrification enhanced by remineralization, causes a decrease in the POM C : N ratio. Degradation of terrigenous POM and bacterial biomass biosynthesis leads to positive deviations in $\delta^{15}\text{N}$ and $\delta^{13}\text{C}$. Relatively refractory hydrocarbons, aromatic compounds, and phenols are accumulated by microbial processes in this system. This study provides mechanistic insights into the missing chemical and isotopic signals and microbially driven fate of terrigenous POM in the ocean, with important implications for how riverine material input affects marine carbon and nitrogen cycling.

*Correspondence: yaozhang@xmu.edu.cn; jiao@xmu.edu.cn

This is an open access article under the terms of the [Creative Commons Attribution-NonCommercial-NoDerivs](https://creativecommons.org/licenses/by-nc-nd/4.0/) License, which permits use and distribution in any medium, provided the original work is properly cited, the use is non-commercial and no modifications or adaptations are made.

Additional Supporting Information may be found in the online version of this article.

Author Contribution Statement: Y.Z. and N.J. conceived and designed the study. M.C., L.Z., and Y.Z. analyzed all data and wrote the manuscript with the help of all authors. L.Z., J.W., X.X., X.C., C.H., and H.T. performed the experiments. Y.Z. performed metagenomic binning to obtain metagenome-assembled genomes. X.N. and M.Z. performed ^{14}C isotope analysis. All authors discussed the results and contributed to the final version of the paper. Lianbao Zhang and Mingming Chen contributed equally to this work.

Ongoing climate change is expected to lead to increased global river runoff (Labat et al. 2004; Andersson et al. 2015). Both ecological modeling and field research have indicated that the flux of terrestrial input to oceans increases with increased river runoff (Andersson et al. 2015). However, few molecular signals of abundant terrestrial organic matter are detected in marine environments (Hedges et al. 1997; Bianchi 2011; Kandasamy and Nath 2016), and only a trace of terrigenous organic matter (e.g., lignin) is present in the ocean (Opsahl and Benner 1997). A proposed explanation for this is a priming effect, in which the addition of labile organic carbon increases remineralization of the relatively refractory organic carbon (Bianchi 2011; Morling et al. 2017). Mineralogical composition and characteristics have also been proposed as important factors controlling the fate of continentally

derived organic matter in the ocean (Blattmann et al. 2019). The essential mechanism behind these explanations is whether and how microbes process terrigenous organic matter, although some nonbiological transformation via photo-oxidation and autoxidation (Galeron et al. 2015) may also contribute. To date, the underlying coupled geochemical, molecular, and genetic information associated with this essential mechanism remains unknown, hindering understanding of the fate of terrigenous organic matter in oceans.

Terrigenous particulate organic matter (POM) is an important form of terrestrial input, accounting for approximately 40% of total terrestrial organic carbon flux to the ocean (Hedges et al. 1997). Terrigenous POM, which mainly originates from vascular plants, contains abundant nitrogen-free biomacromolecules, and has a high carbon to nitrogen molar ratio (C : N; 20–500) (Hedges et al. 1997). Conversely, marine POM generally has a much lower, constant C : N ratio (~6.6) based on the classical Redfield ratio (Redfield 1934; Redfield et al. 1963). Terrestrial plants, most of which fix carbon via the Calvin–Benson pathway, have a lower $\delta^{13}\text{C}$ value (–28‰ to –25‰) than temperate marine phytoplankton (–24‰ to –18‰) (Fry and Sherr 1989; Goericke and Fry 1994). This is because the latter can take up more HCO_3^- , which has higher $\delta^{13}\text{C}$ values than CO_2 (Chapelle and Knobel 1985; Lamb et al. 2006). Similarly, terrigenous POM generally has low $\delta^{15}\text{N}$ values (<5‰) (Thornton and McManus 1994; Riera et al. 2000; Guo and Macdonald 2006) because of the prevalence of nitrogen fixation on land (Peters et al. 1978), whereas substantial variations in $\delta^{15}\text{N}$ values are detected in marine organic materials of different origins and stages of degradation (Hedges et al. 1997). The C : N ratio of POM dramatically decreases from rivers to estuaries (Wu et al. 2007; Huang et al. 2018), then slowly increases from the coastal to open ocean (Wu et al. 2007; Huang et al. 2018; Zhang et al. 2020), whereas the values of $\delta^{13}\text{C}$ and $\delta^{15}\text{N}$ of POM increase from rivers to the ocean (Hedges et al. 1997; Zhang et al. 2020). Although such changes may be attributed to the direct physical mixing of POM originating from rivers and the ocean (Sugimoto et al. 2006; Zhang et al. 2020), microbially driven processes are of particular interest in these transformations. For example, photosynthesis, biosynthesis, respiration, remineralization, nitrogen fixation, nitrification, denitrification, and assimilation of dissolved inorganic nitrogen (DIN) can all cause variation in C and N stable isotope compositions in bulk POM (Peterson and Fry 1987; Casciotti 2016), and the preferential degradation of organic matter and production of bacterial biomass can result in alteration of the C : N ratio in bulk POM (Thornton and McManus 1994; Thomas et al. 1999; Bourgoin and Tremblay 2010). In natural environments, the physical mixing and microbial processes are concurrent (Cloern et al. 2002), which obscures recognition of microbially driven biogeochemical processes.

Using the Aquatron Facility at Dalhousie University, Canada (Supporting Information Fig. S1), we conducted an

ultra-large-volume (~117,000 liters), long-term incubation experiment simulating the input of riverine water (~20,000 liters) into the ocean with the formation of stratification to explore the microbially controlled fate of terrigenous particles in marine systems. The Ingraupport River derived from forest areas was chosen as the freshwater source; dissolved organic matter (DOM) in such systems is generally dominated by biologically recalcitrant DOC (in a specific environmental context) (RDOct) (Jiao et al. 2018). Time-series analyses of the stable carbon and nitrogen isotope compositions, C : N ratio, and pyrolysis-derived compound components of POM, as well as the microbial community structure and function, were performed in three vertical zones—a river zone (RZ), pycnocline zone (PZ), and seawater zone (SZ)—during an 80-d incubation period after riverine water input. Results provide evidence for the preferential degradation of high carbon compounds by microbes, with subsequent intensive nitrification causing change in terrigenous POM chemical and isotopic characteristics, yielding mechanistic insight into the fate of terrigenous POM in the ocean.

Materials and methods

Experimental system setup, sampling, and basic parameter measurement

The Aquatron facility (<https://www.dal.ca/dept/aquatron.html>) at Dalhousie University, Canada, is 10.64 m height, 3.66 m in diameter, and has a volume of ~117,000 liters. The tank was filled with ~80,000 liters of coastal seawater obtained from Halifax Harbour on 23 September 2017, and prefiltered through 300- μm pore-size bolting cloth. The system was kept in the dark to stabilize for 80 d to remove excess organic matter produced by phytoplankton and to inhibit residual photoautotroph activity, after which ~20,000 liters of riverine water collected from the Ingraupport River was prefiltered with 300- μm pore-size bolting cloth and gently added to the seawater surface on 12 December 2017. Incubation was performed in the dark. Time-series samples for analyses of POM, biological oxygen demand (BOD₅), chemical oxygen demand (COD_{Mn}), dissolved oxygen (DO), dissolved inorganic carbon (DIC), nutrients, 16S rRNA genes and transcripts, and metagenomes, were collected from each of the RZ, PZ, and SZ in accordance with the sampling schedule presented in Supporting Information Table S1. The ultra-large-scale simulation of this experiment precluded replication. However, previous studies have indicated a high reproducibility of biogeochemical parameters, microbial abundance, and phytoplankton diversity among the replications in mesocosm experiments (11,000 liters \times 3 replicates in Engel et al. 2005; 3000 liters \times 5 replicates in Huang et al. 2021).

A Multiparameter Sonde (YSI EXO, YSI Inc.) was used to record temperature and salinity. Density was calculated based on the thermodynamic equation of seawater—2010 (<http://www.teos-10.org/>). Water samples for nutrient measurements were filtered through 0.45 μm pore-size polyvinylidene fluoride filters (Millipore) and then stored at –20°C until analysis.

Concentrations of ammonium, nitrite, nitrate, phosphate, and silicate were measured using a Skalar SAN⁺⁺ autoanalyzer at Dalhousie University (precisions: ± 0.14 , ± 0.01 , ± 0.14 , ± 0.03 , and $\pm 0.04 \mu\text{mol L}^{-1}$, respectively). DO concentrations were determined using the Winkler method (Carpenter 1965). BOD5 was obtained from the difference in DO before and after a 5-d dark incubation period (Grigoryeva et al. 2020). Samples for DIC analysis were collected into 500-mL glass bottles with ground-glass stoppers, after which mercuric chloride was injected into the water to halt biological activity (Dickson et al. 2007). DIC concentrations were analyzed by coulometric titration using a VINDTA 3C (Marianda) as described by Dickson et al. (2007) (precision: $\pm 2\text{--}3 \mu\text{mol kg}^{-1}$).

Stable C and N isotope, C : N ratio, ^{14}C , and compound components of POM

Water samples for POM were collected on 0.7- μm pore-size GF/F filters that had been precombusted at 450°C for 4 h (47 mm diameter; Whatman) and then stored at -20°C until analysis. Filters were freeze-dried, fumed with concentrated hydrochloric acid vapor for 48 h, washed with Milli-Q water, and then dried at 60°C until constant weight. Particulate organic carbon (POC) and particulate organic N concentrations and isotopic composition ($\delta^{13}\text{C}$ and $\delta^{15}\text{N}$) of particulate matter were measured using a continuous-flow elemental analyzer (Flash 152 EA 1112 HT) coupled with an isotope ratio mass spectrometer (Thermo Finnigan Delta V Advantage, Thermo Fisher Scientific). C and N isotope ratios ($^{13}\text{C}/^{12}\text{C}$ and $^{15}\text{N}/^{14}\text{N}$) were calibrated to working standards and presented using δ notation (units per mil [‰]) as described by Zhang et al. (2016). The precision of the isotope ratio determinations was 0.2‰ and 0.25‰ for $^{13}\text{C}/^{12}\text{C}$ and $^{15}\text{N}/^{14}\text{N}$, respectively.

POM ^{14}C contents were measured at the Ocean University of China radioCarbon Accelerator Mass Spectrometer Center (OUC-CAMS) in Qingdao, China, using an Accelerator Mass Spectrometer (MICADAS, Ionplus AG) interfaced to an Elemental Analyzer, in which CO_2 gas was injected into the ion source of MICADAS through the Gas Interface System. All ^{14}C measurements were reported as fraction modern (Fm) or $\Delta^{14}\text{C}$, and the conventional radiocarbon ages (year before present) were calculated using the Libby half-life. The precision for $\Delta^{14}\text{C}$ measurements was 8–10‰. Pyrolysis-derived components of POM were analyzed using chromatography-mass spectrometry as previously described (Çoban-Yıldız et al. 2006; Zhang et al. 2016) (Supporting Information).

Microbial community composition and metagenomic analysis

For microbial community composition analysis, water samples (0.75–4 liters) were successively filtered through 3-, 0.8-, and 0.2- μm pore-size polycarbonate membranes (Millipore) at a pressure of $< 0.03 \text{ MPa}$. All membranes were stored in 2-mL RNase-free tubes. Samples for RNA extraction were further filled with 1.5 mL RNeasy lysis buffer (RNA stabilization solution,

Ambion) at -20°C . For metagenomics analysis, 12.5–60 liters water was successively filtered through 0.8- and 0.2- μm pore-size polycarbonate membranes (142 mm diameter), after which membranes were stored at -20°C until DNA extraction. Detailed information on nucleic acid extraction, 16S rDNA and rRNA sequencing and downstream analysis, metagenomic sequencing, assembly, binning, classification, and function annotation are provided in Supporting Information.

Statistical analyses and calculations

Differences between groups of data were tested using the non-parametric Wilcoxon test with the vegan package in R because data were not always normally distributed. Redundancy analysis (RDA) was conducted based on the relative abundances of bacteria and the Z-transformed biogeochemical parameters using the vegan package in R to analyze variations in bacterial communities at the phylum level under the constraint of biogeochemical factors. The null hypothesis that the bacterial assemblage was independent of environmental parameters was tested using constrained ordination with a Monte Carlo permutation test (999 permutations). Significant explanatory parameters ($p < 0.05$) without multicollinearity (variance inflation factor < 10) (Cao et al. 2019) were obtained. Standard and partial Mantel tests were run in R to determine correlations between particle parameters and bacterial community compositions. Dissimilarity matrices of communities were based on Bray–Curtis distances between samples, and particle parameters were based on Euclidean distances between samples. The significance of the Mantel test based on Spearman correlations was obtained after 999 permutations. Principal component analysis (PCA) was conducted based on the Z-transformed relative abundance of metagenomic reads using the vegan package in R to analyze the degradation characteristics of organic substrates over the course of the experiment. For network analyses, Spearman's rank correlations among the relative abundances of metagenomic reads belonging to different microbial groups (phylum level), metagenomic reads involved in degradation of different substrates, and different pyrolysis-derived components, were calculated in R. Only statistically significant ($p < 0.05$) correlations were considered as valid co-occurrence events. Networks were visualized using Cytoscape v3.7.2 (Shannon et al. 2003). A two end-member mixing model was performed for the prediction of POM compound and elemental compositions in PZ and SZ caused by direct physical mixing (Supporting Information).

Results

Changes in biogeochemical profiles during incubation

The temperature during incubation decreased slightly from 18.7°C to 15.7°C in RZ, and 18.3°C to 16.5°C in SZ. Throughout the experiment, low ($\sim 0\text{‰}$) and high ($\sim 33\text{‰}$) salinity values were maintained in RZ and SZ, respectively, indicating that the water was well stratified in the Aquatron tower (Fig. 1a; density values are shown in

Supporting Information Fig. S2). DO concentration decreased during incubation and was significantly higher in RZ (9.0–9.5 mg L⁻¹) than in either PZ (7.0–8.1 mg L⁻¹) or SZ (6.4–

7.4 mg L⁻¹) (Wilcoxon test, $p < 0.01$; Fig. 1b). Conversely, the concentration of DIC was much lower in RZ (83–93 $\mu\text{mol kg}^{-1}$) than in either PZ (791–1666 $\mu\text{mol kg}^{-1}$) or SZ

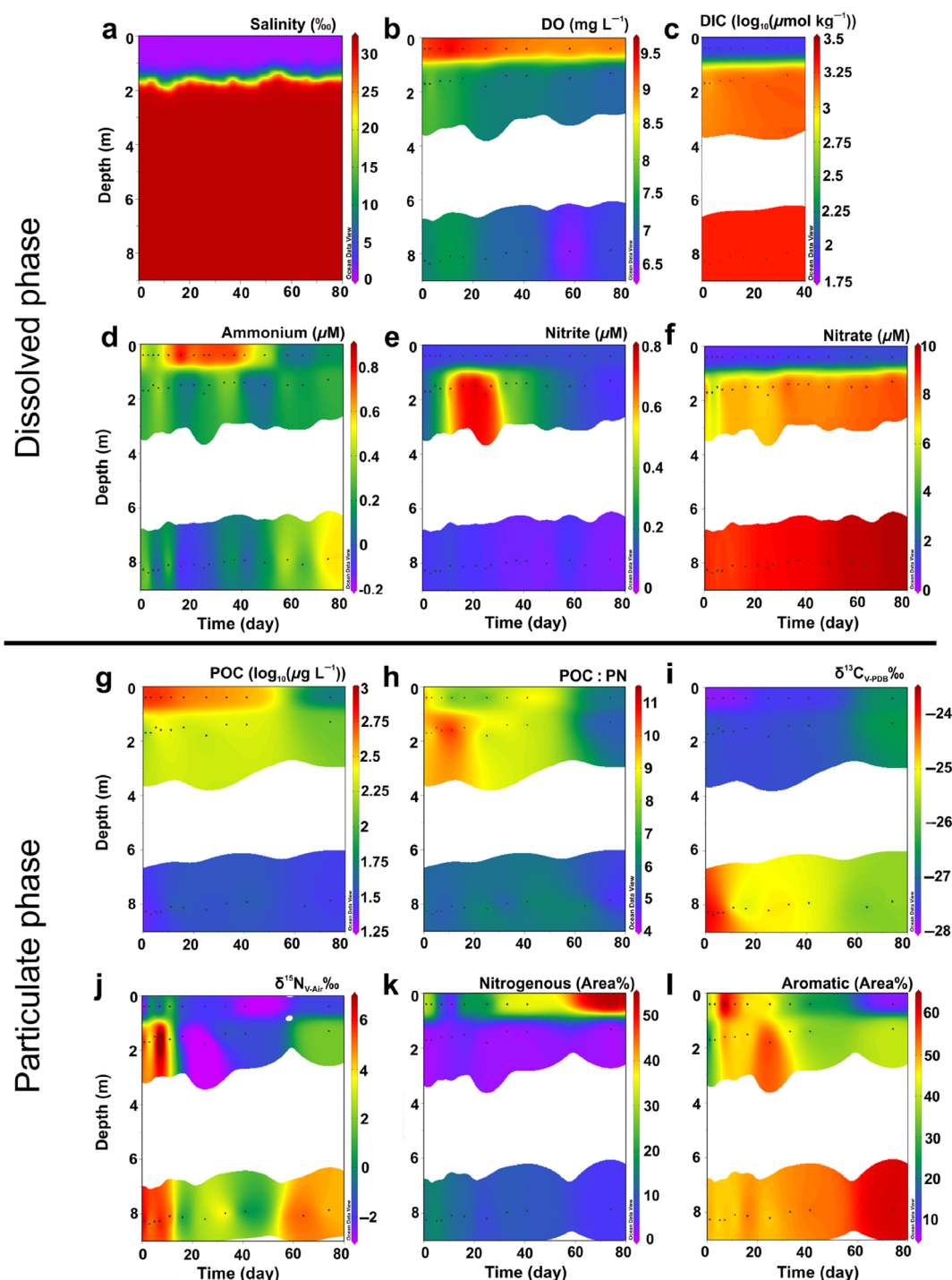


Fig. 1. Biogeochemical properties during incubation in the river-seawater stratified incubation system. (a) Salinity, concentrations of (b) DO, (c) DIC, (d) ammonium, (e) nitrite, (f) nitrate, (g) POC, (h) atomic ratio of C to N (POC : PN), (i) $\delta^{13}\text{C}$ and (j) $\delta^{15}\text{N}$ of POM, (k) contents (area%) of pyrolysis-derived nitrogenous compounds, and (l) aromatic compounds. Contour plots were created in Ocean Data View (<https://odv.awi.de>). Black dots in each panel represent measured values.

(1988–2001 $\mu\text{mol kg}^{-1}$) ($p < 0.01$; Fig. 1c). Concentrations of ammonium, nitrite, and nitrate also showed distinctly different distributions. Specifically, ammonium and nitrite were concentrated in RZ (0.6–0.8 μM) and PZ (0.4–0.8 μM), respectively, from days 11 to 37, whereas high nitrate concentrations occurred in SZ throughout the experiment (increasing from 8.8 to 9.9 μM) (Fig. 1d–f). There was also a slow increasing trend of nitrate in RZ (0.8–1.4 μM) and in PZ (7.8–8.5 μM) (Fig. 1f) and of ammonium (0–0.6 μM) in SZ over the course of the experiment (Fig. 1d).

The concentration of POC was highest in RZ (to 645 $\mu\text{g L}^{-1}$) at the beginning of incubation, displaying a prominent terrigenous input into the system, but dropped to 50 $\mu\text{g L}^{-1}$ by the end of the incubation period (Fig. 1g). In PZ and SZ, POC concentrations were much lower, but they briefly rose during the early incubation stage, with maximums occurring on days 5 and 11, respectively. In general, the molar ratio (C : N) of POC to particulate nitrogen (PN) decreased in the three zones during incubation. In addition, the ratio was significantly higher in RZ (5.8–10.5) and PZ (5.4–11.3) than it was in SZ (4.4–6.5; $p < 0.01$; Fig. 1h). In PZ, a distinct increase in C : N (10.1–11.3) was observed between days 5 and 11. The particulate $\delta^{13}\text{C}$ was clearly lower in RZ and PZ (–28‰ and –27‰, respectively) than in SZ (–24‰) at the beginning of the experiment. During incubation, the $\delta^{13}\text{C}$ increased in RZ and PZ, but it decreased in SZ, and it tended to be homogeneous throughout the water column at the end of the incubation period (Fig. 1i). Particulate $\delta^{15}\text{N}$ was highest at the beginning of the experiment throughout the water column. In RZ, $\delta^{15}\text{N}$ gradually decreased during incubation, whereas it first decreased and then increased in PZ and SZ, with minima occurring on days 24 and 41, respectively (Fig. 1j).

Nitrogenous and aromatic organic compounds displayed opposite trends throughout the experiment (Fig. 1k,l). In RZ and PZ, the proportion of nitrogenous compounds generally continued to increase while that of aromatic compounds decreased over the course of the experiment; however, the opposite trend was observed in SZ. The maximum relative contents of nitrogenous and aromatic compounds occurred at the end of the experiment in RZ and SZ, respectively (Fig. 1k,l).

Succession in bacterial and archaeal communities

Proteobacteria were dominant in both bacterial 16S rDNA and rRNA amplicons obtained from RZ and PZ throughout the experiment (Fig. 2a). Rhodospirillales was among the most abundant of orders within Proteobacteria in all three zones, whereas the orders Burkholderiales and Rhizobiales were only abundant in RZ and Oceanospirillales and Rhodobacterales were only abundant in PZ and SZ (Supporting Information Figs. S3, S4). Operational taxonomic units (OTUs) assigned to Actinobacteria, Verrucomicrobia, and Acidobacteria were more abundant in RZ than in other zones (Wilcoxon test, $p < 0.01$),

whereas OTUs assigned to Bacteroidetes were more abundant in PZ ($p < 0.01$). There was a slight decreasing trend in the relative abundance of Actinobacteria within the bacterial 16S rDNA amplicons from RZ during the experiment. The relative abundance of Bacteroidetes was highest on day 11 in the 0.2–0.8 and 0.8–3 μm size fractions of both 16S rDNA and rRNA amplicons from PZ (Fig. 2a). Actinobacteria and Bacteroidetes were more abundant in the 0.2–0.8 μm size fraction than in the larger size fractions ($p < 0.05$ or 0.01). In contrast, OTUs assigned to Planctomycetes were clearly enriched in the 0.8–3 and >3 μm size fractions. Notably, in SZ, Proteobacteria were dominant in the 0.2–0.8 μm size fraction, but Planctomycetes was the most abundant group in the 0.8–3 and >3 μm size fractions for both the 16S rDNA- and rRNA-based libraries (Fig. 2a). Archaeal communities were dominated by Thaumarchaeota, mainly those belonging to ammonia-oxidizing Marine Group I (Fig. 2b). Analysis of nitrite-oxidizing bacteria (NOB) revealed that active Nitrospirae were mainly distributed in RZ whereas Nitrospinae were enriched in PZ and SZ (Fig. 2c; see detailed descriptions in Supporting Information).

Variations in metabolic functions of prokaryotic communities

Functional profiling of metagenomes showed that the reads were primarily associated with pathways involved in carbohydrate and amino acid metabolism, genetic information processing, and environmental information processing (Supporting Information Fig. S5). In SZ, the relative abundances of reads associated with amino acid metabolism, metabolism of cofactors and vitamins, nucleotide metabolism, and energy metabolism were higher in the 0.2–0.8 μm size fraction than in the >0.8 μm size fraction (Wilcoxon test, $p < 0.01$). In contrast, the relative abundances of reads associated with carbohydrate metabolism and lipid metabolism were higher in the metagenomes from the >0.8 μm size fraction ($p < 0.01$). Notably, the relative abundance of reads associated with amino acid metabolism displayed an inverse trend over the course of the experiment when compared with carbohydrate metabolism, but was similar to that of reads associated with energy metabolism in SZ. For instance, the relative abundance of reads associated with amino acid metabolism in the 0.2–0.8 μm size fraction of SZ was lowest (11.2%) on day 11, whereas that of reads associated with carbohydrate metabolism was at its highest level (10.0%). In the >0.8 μm size fraction of SZ, the lowest abundance (9.5%) of reads associated with amino acid metabolism occurred on day 16, when the highest abundance of reads associated with carbohydrate metabolism (10.7%) was obtained (Supporting Information Fig. S5). Metagenome-assembled genome (MAG)-level results showed similar variations in metabolic functions (Supporting Information).

To clarify the processes from POM remineralization to downstream nitrogen-cycling in this system, the metagenomic

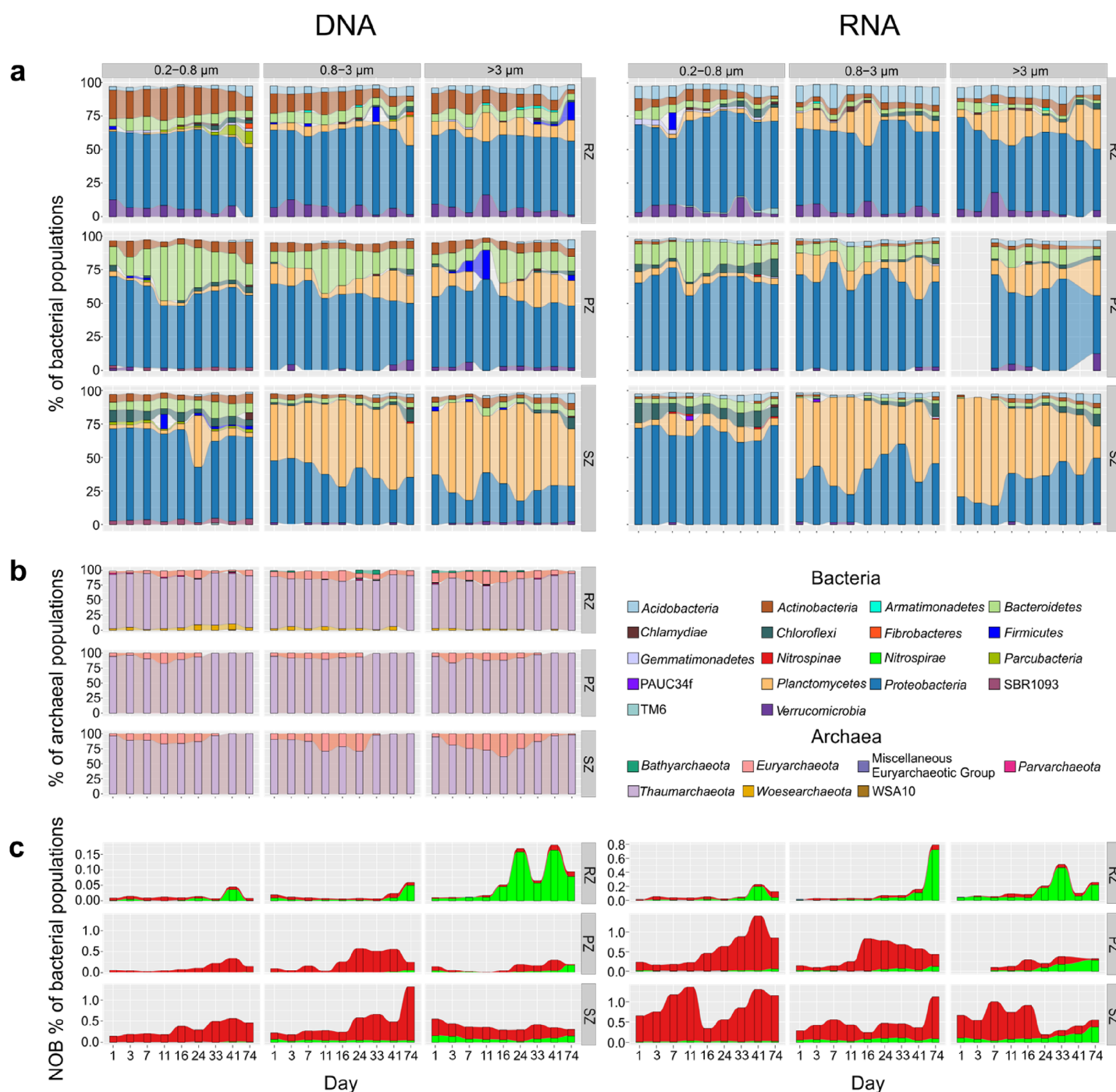


Fig. 2. Size-fractionated microbial community composition during incubation. **(a)** Bacterial community, **(b)** archaeal community, and **(c)** NOB are shown at the phylum level based on 16S rDNA (left) and rRNA (right) libraries. In **(a)** and **(b)**, only populations with a relative abundance of >1% in at least one 16S rDNA- or rRNA-based library are shown.

reads associated with CAZymes, peptidases, C-fixation, and N-cycle-related genes were further analyzed (Fig. 3). The taxonomic compositions of gene reads encoding CAZymes and peptidases were generally constant throughout the experiment for each size fraction in SZ. The reads encoding CAZymes and

peptidases had higher relative abundances in the 0.2–0.8 μm size fractions than in the >0.8 μm size fractions, and their ratios (CAZ : pep) were notably higher in the > 0.8 μm size fractions in PZ and SZ (Fig. 3; $p < 0.01$). The majority of reads encoding CAZymes and peptidases were assigned to Proteobacteria and

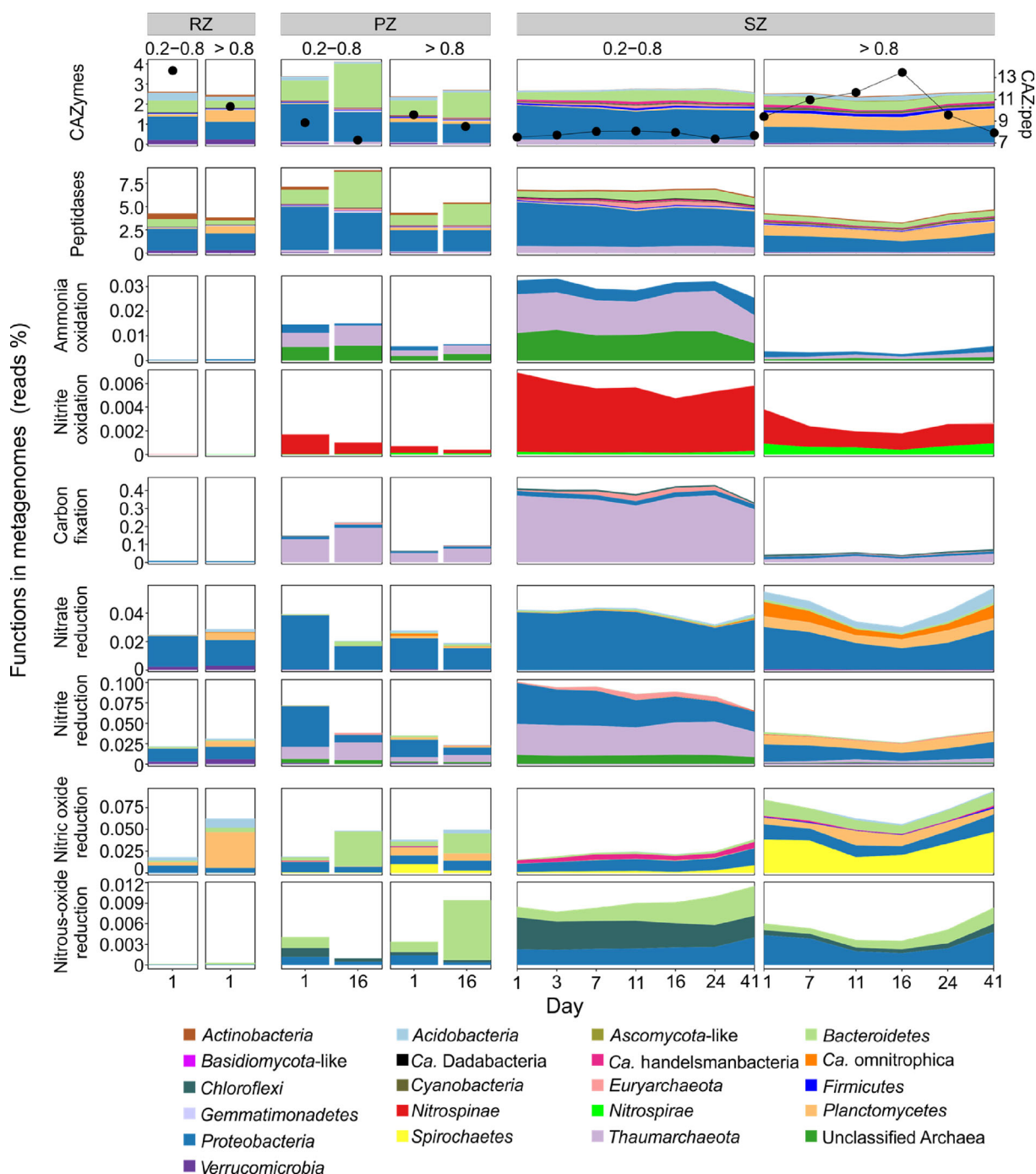


Fig. 3. Variations in taxonomic composition of metagenomic reads across different incubation times (day). Relative abundances of reads involved in carbohydrate-active enzymes (CAZymes), peptidases, ammonia oxidation (*amo*), nitrite oxidation (*nrx*), carbon fixation (genes involved in KEGG pathway Ko00720), nitrate reduction (*nar*, *nqr*, *nas*, *NR*), nitrite reduction (*nir*), nitric oxide reduction (*nor*), and nitrous-oxide reduction (*nos*) in the 0.2–0.8 μm and >0.8 μm size fractions of the RZ, PZ, and SZ; only populations with a relative abundance >0.01% in at least one metagenomic library are shown. Ratios of CAZymes to peptidases (CAZ : pep) are shown with black dots.

Bacteroidetes; however, reads assigned to Planctomycetes were also abundant in the >0.8 μm size fractions, especially in RZ and SZ. In PZ, reads assigned to Bacteroidetes accounted for a higher proportion of CAZymes and peptidases-related reads than in RZ

and SZ ($p < 0.01$), especially on incubation day 16 (Fig. 3). Downstream nitrification and C-fixation-related reads showed distinctly higher relative abundances in SZ than in RZ, while relative abundances of denitrification-related reads were similar

in SZ and RZ (Fig. 3; details were described in Supporting Information).

Discussion

Microbial processing of terrigenous POM

The input of riverine water to seawater introduced abundant RDOC and terrestrial particles. Whereas RDOC is relatively recalcitrant to microbial degradation, terrigenous POM can be transformed by microorganisms. As indicated by the time–depth profile of the POC concentration (Fig. 1g), these particles had sunk to PZ around day 7 and to the bottom of SZ on day 11, which was when POC concentrations first peaked in each zone. Bacteroidetes, Planctomycetes, and Proteobacteria were the major decomposers of POM because they encoded large numbers of genes coding for CAZymes and peptidases, especially in size fractions associated with particles. The increasing ratio of CAZymes to peptidases (CAZ : pep) from days 11 to 16 in SZ (Fig. 3) suggests that microorganisms tended to degrade carbohydrate compounds in the presence of a mass of terrigenous POM. This was supported by the coupled analysis of the pyrolysis-derived components of POM, microbial community composition, and metagenomics-based substrate degradation potential (Fig. 4).

At the beginning of the incubation period, microbial communities in the $>0.8 \mu\text{m}$ size fractions preferentially encoded genes involved in degradation of low-molecular-weight nitrogenous compounds such as amino acids, nucleotide bases, and vitamins (Fig. 4a). With particle input, the community shifted towards encoding genes involved in the degradation of high C : N ratio high-molecular-weight polymers such as pectin and glycosaminoglycan, which are generally derived from vascular plants or animals (Wakeham and Canuel 2006). After day 16, the community resumed preferentially encoding genes involved in the degradation of low-molecular-weight organic matter. These alterations in substrate usage suggest rapid microbial processing of terrigenous POM following oceanic input, explaining the oceanographic enigma in which little terrestrially derived organic matter is preserved in global oceans, despite the considerable annual contribution of fresh riverine organic matter into them (Hedges et al. 1997; Bianchi 2011; Seidel et al. 2015). Notably, most bacterial groups in the $>0.8 \mu\text{m}$ size fractions showed consistent trends over time, with the highest relative abundances occurring on either days 1 or 41 and the lowest on day 16. These findings corresponded to genes involved in degrading low-molecular-weight organic matter being enriched on days 1 and 41, whereas those involved in degrading high-molecular-weight matter were enriched on days 11 and 16 (Fig. 4a). Indeed, the majority of bacterial groups showed significantly positive correlations with genes involved in degrading low-molecular-weight substrates. However, for the Ascomycota- and Basidiomycota-like groups, the highest abundances

occurred on day 16 (Fig. 4a), and these were negatively correlated to most genes involved in degrading low-molecular-weight substrates (Fig. 4c). Moreover, only the Ascomycota-like group positively correlated with genes involved in degrading high-molecular-weight glycosaminoglycan. Metagenomic data notably revealed the relative abundances of Ascomycota-like (0.24%) and Basidiomycota-like (0.02%) groups in particles in RZ to be not higher than those in SZ (0.31% and 0.02%, respectively) at the beginning of this experiment, indicating that their increase in SZ on day 16 did not result from the physical mixture of seawater and sinking of terrigenous matter. Ascomycota and Basidiomycota can both degrade terrigenous plant biomass, including polysaccharides (cellulose, hemicellulose, and pectin) and lignin (Pelaez et al. 1995; Couturier et al. 2016). Therefore, the increase of the Ascomycota- and Basidiomycota-like groups in SZ on day 16, as well as their significantly positive correlations with many pyrolysis-derived ester components, may reflect their decomposition of high-molecular-weight and high C : N ratio terrigenous POM (Fig. 4c). We speculate that these low-abundance fungi-like groups likely act as pioneers in the processing of terrigenous particulate materials in the ocean, leaving the low-molecular-weight nitrogenous organic matter to be degraded by Planctomycetes and Proteobacteria. The taxonomy and role of these fungi-like groups need to be confirmed by further work.

POM can also significantly influence the free-living bacterial community (Kiorboe and Jackson 2001; Azam and Malfatti 2007; Zhang et al. 2016). In this system, variations in the relative abundances of genes involved in degrading different substrates with time in the $0.2\text{--}0.8 \mu\text{m}$ size fractions were generally similar to those in the $>0.8 \mu\text{m}$ size fractions, but a finer-scale succession pattern of these genes was observed (Fig. 4b). At the beginning of the incubation period, the microbial community tended to encode genes involved in degrading monosaccharides and derivatives. However, between days 7 and 16, the community tended to encode more genes involved in the degradation of the terrigenous high-molecular-weight components glycosaminoglycan and pectin than on other days with input of the sinking terrestrial particles ($p < 0.01$). After day 16, the potential for degradation of small nitrogenous molecules such as nucleotide bases increased with decreasing influence from the sinking particles. Relationships among POM components, microbial community composition, and degradation-related genes in the $0.2\text{--}0.8 \mu\text{m}$ size fractions were more complex than in the $>0.8 \mu\text{m}$ size fractions, as indicated by the greater number of POM components in the network (Fig. 4d). This suggests a more cooperative interaction and distinct metabolic division of labor among different free-living microbial groups during the degradation of various substrates. We speculate that terrigenous POM directly supplied substantial substrates for many particle-attached microbial groups, alleviating their competition for a substrate, as indicated by the compact and polarized

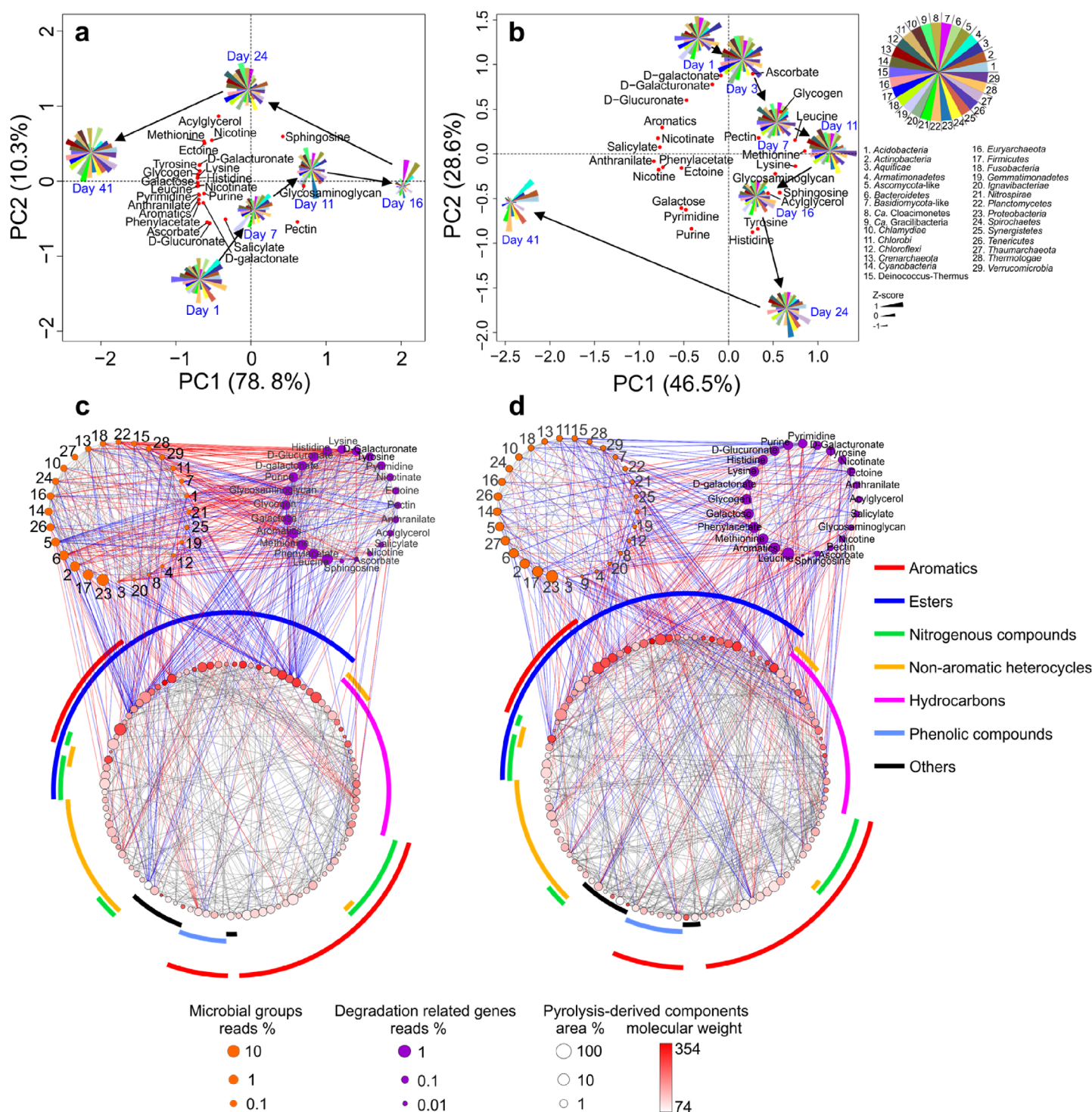


Fig. 4. Coupled analysis of pyrolysis-derived components of POM and microbial metagenomes in the SZ. **(a)** PCA of the compositions of metagenomic reads involved in degrading different substrates in the >0.8 and **(b)** $0.2\text{--}0.8$ μm size fractions. **(c)** Network interactions within and among the relative abundances of metagenomic reads assigned to different microbial groups (phylum level), the relative abundances of metagenomic reads involved in degrading different substrates, and the relative contents of different pyrolysis-derived components in the >0.8 and **(d)** $0.2\text{--}0.8$ μm size fractions. In PCA plots, substrate information is shown beside the red dots and the Z-transformed taxonomic compositions of each sample (based on metagenomic data) are shown using the sector diagram. In network plots, red lines represent positive and blue lines represent negative correlations between datasets; gray lines represent positive/negative correlations within datasets. Top-left, top-right, and lower panels represent the taxonomic groups, metagenomic reads involved in degrading different substrates, and pyrolysis-derived components, respectively. Circle size reflects the relative abundance or content. Circle color reflects the molecular weights of pyrolysis-derived components. C : N is $>$ Redfield ratio of 6.6 in 12 of 17 nitrogenous compounds.

distribution pattern of points representing different substrate-degradation-related genes in the PCA plot (Fig. 4a). However, free-living groups can be forced to utilize their preferred substrates, for which they have higher affinity and the greatest competitive advantage, when there are limited dissolved substrate resources.

Microbial transformation of C : N ratio of POM

Microbial degradation of terrigenous POM and subsequent processes (e.g., nitrification, *see* detailed statements in Supporting Information) triggered by remineralization will alter characteristics of POM such as the C : N ratio, $\delta^{13}\text{C}$, and $\delta^{15}\text{N}$. RDA of the variations in bacterial communities under the constraint of environment parameters revealed that particle-attached Planctomycetes in SZ were generally positively correlated with $\delta^{15}\text{N}$ and negatively correlated with C : N, whereas free-living Proteobacteria and Bacteroidetes displayed the opposite trend. In addition, members of Acidobacteria, Actinobacteria, and Verrucomicrobia in RZ were positively correlated with catabolism-related parameters, including BOD₅, DO, and NH_4^+ concentration (Fig. 5a). Mantel and partial Mantel tests further confirmed the positive correlations between either microbial community compositions or metabolic functions and characteristics of the POM elemental composition (Fig. 5b,c).

The drastic decrease in concentration of POC in RZ, as well as the estimated greater loss of PN (relative to the first day) in RZ and the lower accumulation of PN in SZ than accumulation of DIN in the corresponding zones (Fig. 6a, b), suggests a distinct sinking of POM from RZ to SZ and degradation in SZ. If POM is assumed to be conserved, the pyrolysis-derived components, C and N stable isotope compositions, and C : N ratios of POM can be predicted by a two end-member mixing model. We report large deviations between predicted and measured values (Fig. 6c), suggesting that microbial processes other than physical mixing play an important role in this system. The strongly negative deviation of the POM C : N ratio from the predicted value in SZ and the deviation in the negative direction with incubation time in PZ indicate that high C matter was degraded preferentially and/or high N matter was biosynthesized in this system. For example, esters, non-aromatic heterocycles, and nitrogenous compounds (C : N > 6.6 in 12 of 17 compounds) were preferentially degraded, as shown by distinctly negative deviations from the prediction (Fig. 6c). Comparatively, hydrocarbons, aromatic compounds, and phenols were accumulated by microbial processes in this system, as suggested by the positive deviations (Fig. 6c); this finding is consistent with these materials being relatively refractory in the ocean (Canfield 1994; Jiao et al. 2018; McDonald et al. 2019). It should be noted that polysaccharides, which were actively degraded in response to the input of terrigenous POM based on metagenomic analysis, were not obtained from pyrolysis products. We next use metagenomic

analysis to elucidate the deviation of C : N in response to microbial processes.

Metagenomic data (Supporting Information Figs. S5, S6) reveal that terrigenous POM with high C : N ratios may facilitate the growth of microbial groups preferring C rather than N sources in the upper layers of this stratified system. For example, MAGs affiliated with Actinobacteria and Verrucomicrobia were enriched in carbohydrate metabolism-related genes (Supporting Information Fig. S6), and the two groups had a higher abundance in RZ than in PZ and SZ (Fig. 2a) during the early stages of the incubation. As the experiment continued, the majority of terrigenous particles with high C : N ratios sank from the surface to the bottom, leaving suspended particles as the dominant components of POM in RZ and PZ. Various biogenic entities that formed in situ, such as bacterial and archaeal assemblages, can be important components of suspended particles (Turner and Millward 2002), which was demonstrated well in our study by the low C : N ratio of POM (close to bacterial $\sim 5 : 1$) (Seitzinger and Sanders 1997) in RZ and PZ at the end of this experiment (Fig. 1h).

A mass of sinking terrigenous POM arrived at PZ and SZ on days 7 and 11, respectively (Fig. 1g). Because of the high C : N ratios of this POM, this influx may have reshaped the functional structure of the microbial communities in PZ and SZ toward a preference for carbohydrate metabolism. This was reflected by the higher proportion of metagenomic reads involved in carbohydrate metabolism on days 11 or 16 than at the beginning of this experiment (Supporting Information Fig. S5). In PZ, it is possible that some low-density terrigenous POM remained in the pycnocline while high-density POM sank through it. Low-density POM contains more transparent exopolymer particles consisting predominantly of surface-active polysaccharides with high C : N ratios (Azetsu-Scott and Passow 2004), consistent with our highest measured C : N ratio (to 11.34) and lowest content of pyrolysis-derived nitrogenous compounds being measured between days 7 and 16 in PZ (Fig. 1h,k). These polysaccharides may have fueled the high abundance of Bacteroidetes, which we assume are specialized at degrading high-molecular-weight compounds (Fernández-Gomez et al. 2013) in PZ (Figs. 2a, 3). Indeed, the MAGs assigned to Bacteroidetes contain more genes involved in glycan biosynthesis and metabolism (Supporting Information Fig. S6). Polysaccharide decomposition may contribute to the decreasing C : N ratio with extended incubation time. Because Bacteroidetes had a higher C than N use efficiency in amino acids (Xavier et al. 2013), this may also have led to a preferential degradation of POM, altering it to a lower C : N ratio in PZ over the experimental duration (Figs. 1h, 7c). With the decrease in POM C : N ratio after day 16 in PZ, the relative abundances of Bacteroidetes decreased whereas those of Planctomycetes increased (Fig. 2a), suggesting that Planctomycetes may have utilized the nitrogenous components immediately after the high-C polysaccharides were degraded by Bacteroidetes. This is consistent with the

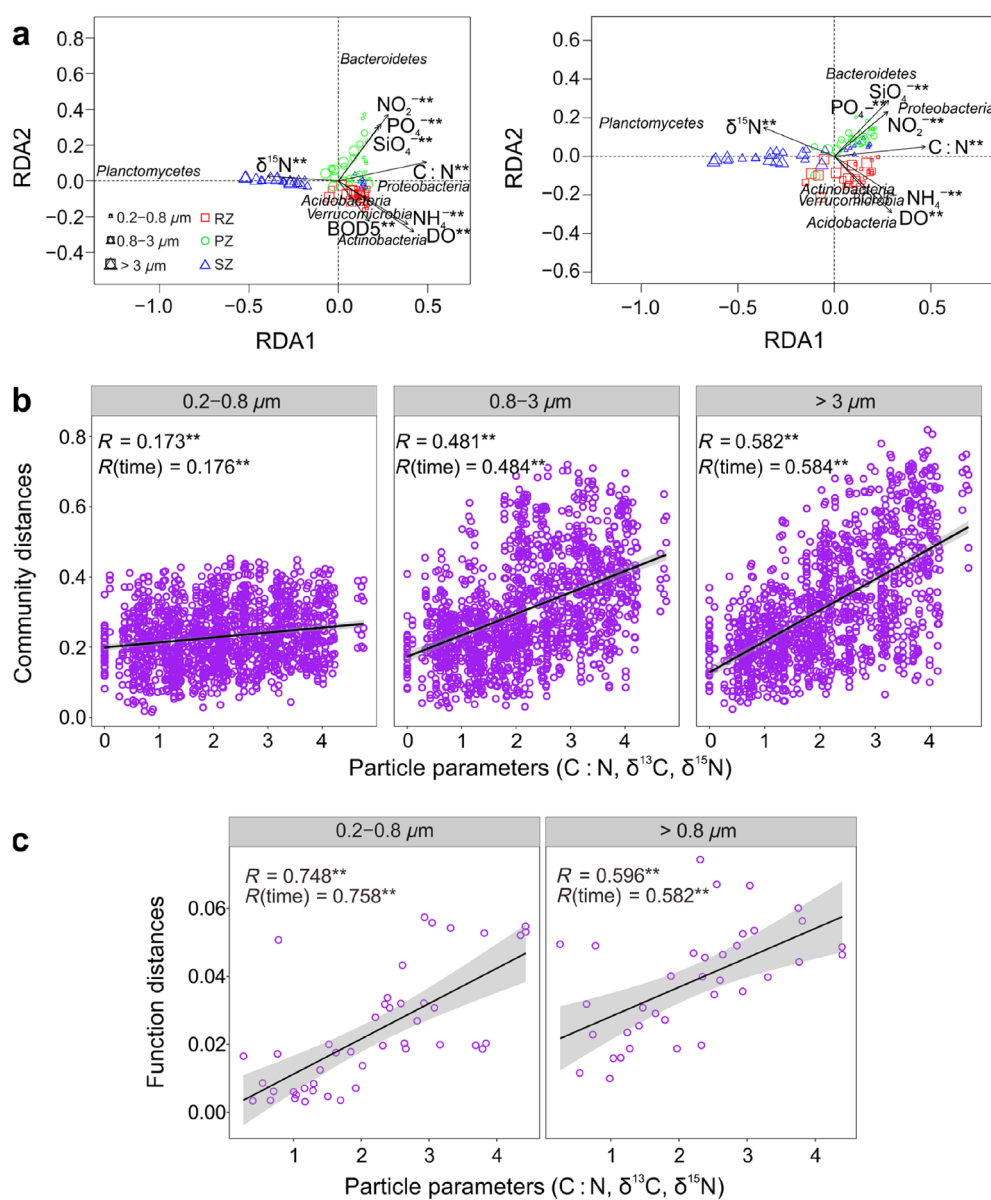


Fig. 5. Correlation analysis of microbial community compositions, metabolic functions, biogeochemical parameters, and characteristics of the POM elemental composition. **(a)** RDA of bacterial communities under biogeochemical constraints based on 16S rDNA (left) and rRNA (right) libraries. **(b)** Correlations between the Bray–Curtis dissimilarities of bacterial community compositions based on 16S rDNA and rRNA based libraries and the Euclidean distances of POM geochemical characteristics (C:N ratio, $\delta^{13}\text{C}$, and $\delta^{15}\text{N}$) between samples. **(c)** Correlations between the Bray–Curtis dissimilarities of metagenomic function compositions based on KEGG pathway annotation and the Euclidean distances of POM geochemical characteristics (C:N ratio, $\delta^{13}\text{C}$ and $\delta^{15}\text{N}$) between samples. Pearson correlation coefficient (R) values are shown for regular and partial Mantel tests in **(b)** and **(c)**. The p values were calculated using the Mantel test statistics estimated from 999 permutations. $**p < 0.01$. Shaded areas show the 95% confidence intervals of the fits.

metagenomic finding that Planctomycetes are closely linked to genes involved in the degradation of low-molecular-weight nitrogenous organic materials (Fig. 4a,c).

In SZ, the increased preference for C rather than N sources after the input of terrigenous POM is reflected by the highest relative abundance of carbohydrate

metabolism-related metagenomic reads (Supporting Information Fig. S5) and the highest CAZ : pep ratio (Fig. 3) on day 16, and may have contributed to the decreased C:N ratio of POM. The C:N ratio reached its lowest value (5.05) in SZ at the end of the experiment (Fig. 1h), which may have been influenced by the accumulation of suspended

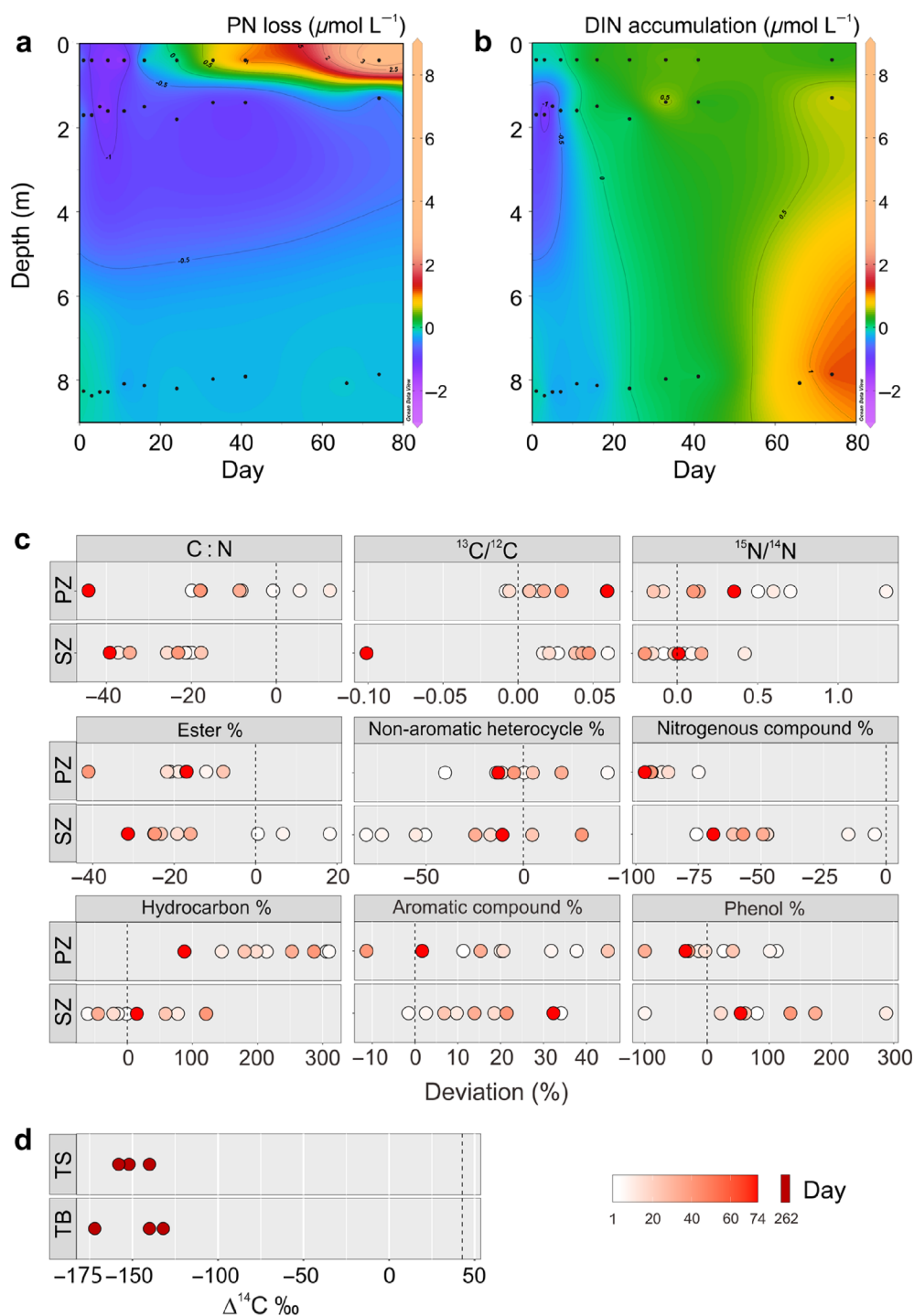


Fig. 6. Mixing versus microbial processing of POM. **(a)** Calculated PN loss and **(b)** DIN accumulation relative to the first day based on the measured concentrations of POC and DIN, and C : N ratio of bulk POM. **(c)** The deviation of measured values from predicted values of biogeochemical parameters of POM based on a two end-member mixing model in the PZ and SZ across different incubation times (day). **(d)** Measured $\Delta^{14}\text{C}$ values (circles) of POM and predicted values (dashed line) based on a two end-member mixing model in the tank surface (TS) and bottom (TB) on day 262 of incubation, when freshwater and seawater were mixed vertically.

biogenic POM with low C : N ratios that was formed in situ by bacteria, archaea, and their secretions (Bayer et al. 2019b). The C : N ratios of bacteria were previously

reported to be $\sim 5 : 1$ (Seitzinger and Sanders 1997) and those of archaea 4–6 (Lorantfy et al. 2014; Bayer et al. 2019a; Meador et al. 2020). Taken together, these

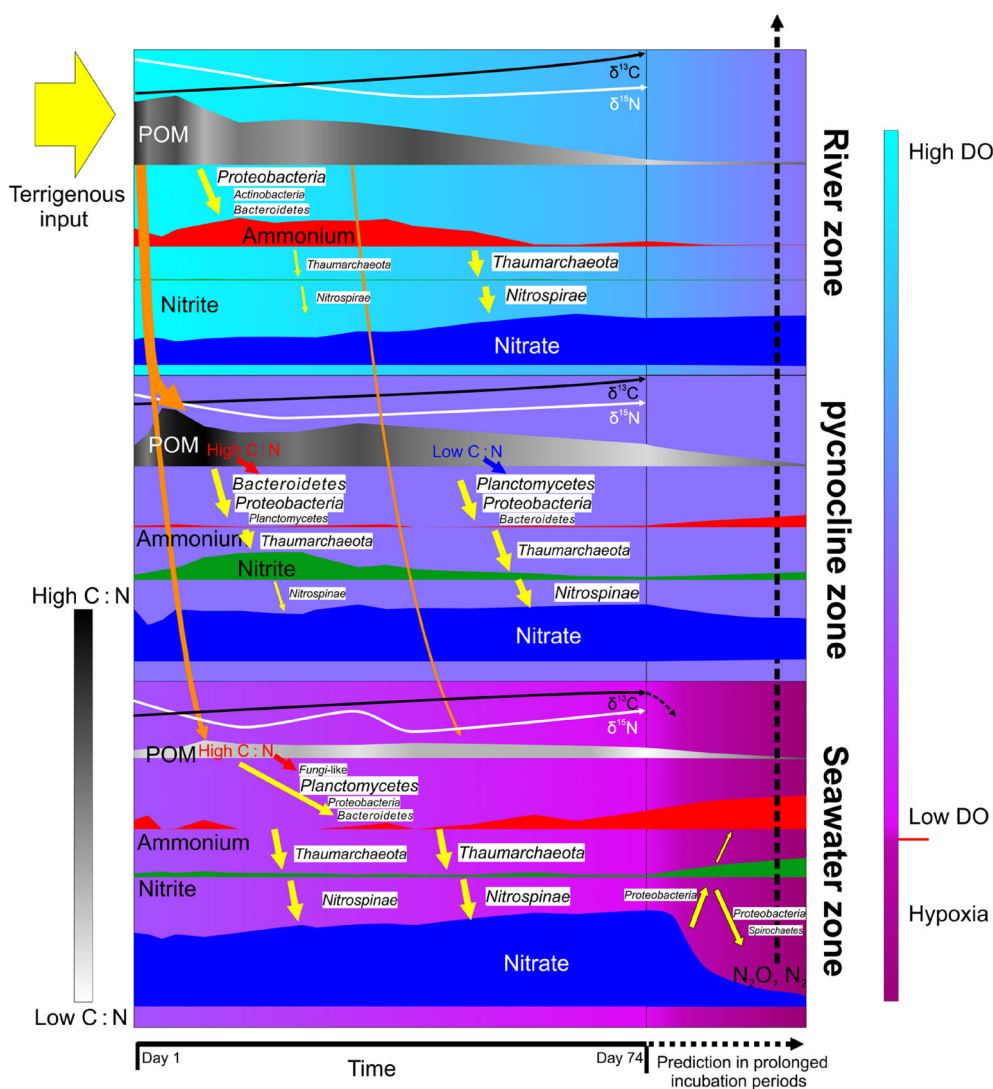


Fig. 7. Overview of microbially driven fate of terrigenous POM in the river–seawater stratified simulation system. Variations in concentrations of nutrients (ammonium, nitrite, and nitrate) and POM, C : N ratio, and isotope compositions of POM within the 74-d incubation period, as well as key microbial groups that play a role in these variations are shown based on measured datasets. The extended portion in the prolonged incubation period after day 74 (dotted x-axis) was inferred based on data analysis. Orange arrows represent POM flux, yellow arrows represent biogeochemical processes, and the vertical dotted arrow represents emission of N_2O and N_2 from the SZ.

findings support the distinct negative deviation of C : N in SZ (Fig. 6c). The microbial degradation of terrigenous POM with high C : N may release high C matter contributing to the higher C : N ratio (~14.4) (Hopkinson and Vallino 2005) of the DOM pool accumulated in the ocean.

Microbial transformation of C and N stable and radiocarbon isotope compositions

Riverine organic matter usually has a lower $\delta^{13}C$ value than marine organic matter because terrestrial organic matter incorporates CO_2 , which has a low $\delta^{13}C$, whereas aquatic phytoplankton takes up HCO_3^- , which has a high $\delta^{13}C$, for biosynthesis (Chapelle and Knobel 1985; Goerick and

Fry 1994; Burkhardt et al. 1999). In the incubation system, the $\delta^{13}C$ value of POM continued to increase in RZ and PZ (Fig. 1i). After most terrigenous sinkable particles had sunk from the surface to the bottom, the remaining suspended POM, which normally has higher $\delta^{13}C$ values than the sinking fraction (Rau et al. 1992), likely contributed to the measured increase of $\delta^{13}C$ in RZ and PZ. Notably, there were slight positive deviations of the $^{13}C/^{12}C$ of POM from those predicted by the mixing model in PZ (Fig. 6c), suggesting an increase in ^{13}C content beyond what physical mixing could account for. We speculate that, with the depletion of terrestrial POM with lower $\delta^{13}C$, bacterial biomass biosynthesis and aggregation, which preferentially utilized ^{13}C -enriched organic substances

(Werth and Kuzyakov 2010), may have resulted in the positive deviation observed in PZ. This was supported by a distinct increase in cell abundance of PZ by up to one order of magnitude (Supporting Information Fig. S7).

The $\delta^{13}\text{C}$ value of POM continued to decrease in SZ (Fig. 1i). The continuous accumulation of sinking particles with low $\delta^{13}\text{C}$ from the upper water may have contributed to this phenomenon. However, there were also slightly positive deviations in $^{13}\text{C}/^{12}\text{C}$ from the mixing model prediction in SZ (Fig. 6c), suggesting that the decrease in ^{13}C content was not as great as predicted. We speculate that greater aggregation of biomass into POM may have been responsible for the slight positive deviation of $^{13}\text{C}/^{12}\text{C}$ from the predicted value in SZ, despite the low cell abundance. The negative deviation of $^{13}\text{C}/^{12}\text{C}$ on the last day of incubation (Fig. 6c) can be attributed to more dominant microbial decomposition of POM, which preferentially consumes ^{13}C -enriched substances (Werth and Kuzyakov 2010) relative to bacterial biomass biosynthesis and aggregation. It is also possible that biomass decreased with C removal by respiration, and/or that chemoautotrophic biosynthesis and aggregation contributed to the negative deviation. It has been suggested that depletion of ^{13}C in ammonia-oxidizing archaea and NOB bulk biomasses is a result of C isotope discrimination by bicarbonate-fixing enzymes (Joachimski 1997; Koenneke et al. 2012). Our research is consistent with this, in a distinct increase in the relative abundances of NOB in the $>0.8\ \mu\text{m}$ size 16S rDNA- and rRNA-based libraries occurred in SZ on the last day (Fig. 2c).

In our system the PN from river water had a lower $\delta^{15}\text{N}$ value than that from seawater (Fig. 1j). Nitrogen isotopic fractionation, which can be caused by almost all N cycle processes, is more complex (Sigman et al. 2009; Casciotti 2016). In general, there were positive deviations in $^{15}\text{N}/^{14}\text{N}$ of PN from the mixing model prediction in PZ, especially during the early stages of incubation, excepting two slightly negative deviations on days 16 and 24 (Fig. 6c). We speculate that remineralization of organic N, in which low- $\delta^{15}\text{N}$ PN was preferentially degraded (Sigman et al. 2009), may have led to the positive deviation in the $^{15}\text{N}/^{14}\text{N}$ in bulk POM, and that bacterial cell biomass biosynthesis by assimilation of organic N and DIN (e.g., NOB) may have led to the negative deviation (Sigman et al. 2009; Casciotti 2016).

The negative deviation of $\Delta^{14}\text{C}\text{‰}$ (-172‰ to -132‰) on day 262 relative to the freshwater (58‰) and seawater sources (-35‰) was observed in prolonged incubation periods (Fig. 6d), suggesting a distinct “aging” effect of POM. This probably was led by microbial preferential degradation of ^{14}C -enriched (i.e., “young”) organic matter (Raymond and Bauer 2001; Bao et al. 2019), such as carbohydrate- and protein-like substances (Loh et al. 2004), or the younger pools of the same class of compounds such as fatty acids (Hou et al. 2021).

Conclusions

We coupled geochemical, molecular, and genetic information from an ultra-large-volume, long-term simulating incubation system. Results clearly reveal the microbially driven fate of terrigenous POM following discharge into marine systems. We create a schematic to illustrate biogeochemical processes transforming terrigenous POM (Fig. 7). In the river–sea water stratified system, sinking terrigenous POM leaves suspended particles in RZ. Analysis of combining the molecular with POM chemical composition data suggests that low-density, high C : N sinking POM were mainly degraded by members of Bacteroidetes in PZ, whereas the high-density, high C : N POM sank to SZ and was degraded by various microbial groups promoting carbon metabolism in SZ. Among these, Planctomycetes may play an important role. Degradation of POM, especially nitrogenous compounds by Planctomycetes, released ammonium and enhanced nitrification by Thaumarchaeota and Nitrospinae/Nitrospirae. Nitrification and the degradation of terrigenous high C : N POM, such as polysaccharides, led to decreased C : N ratios of POM. Isotopic evidence suggests that the selective degradation of the relatively “young” organic matter by microorganisms also led to the “aging” effect of POM. The degradation of terrigenous POM with low $\delta^{15}\text{N}$ may be responsible for the increase of $\delta^{15}\text{N}$ in bulk POM. Whereas POM degradation and chemoautotrophic nitrifiers can enrich ^{12}C in POM, bacterial biomass biosynthesis can enrich ^{13}C after exhaustion of terrigenous POM with low $\delta^{13}\text{C}$, leading to the positive deviation observed in $\delta^{13}\text{C}$. Negative deviations of $\delta^{13}\text{C}$ in bulk POM could occur when chemoautotrophic nitrifier biomass accumulates (e.g., in the low DO environment). The dark and stratified incubation in this study may limit extrapolation of results to real irradiated and dynamic estuarine environments, where photoautotrophy, photo-oxidation, and mixing can be important factors changing terrigenous POM characteristics and affecting microbial degradation. Nevertheless, by removing interference from these factors, we provide a more detailed understanding of, and mechanistic insights into, microbially driven changes in terrigenous POM chemical and isotopic characteristics. Results presented herein have important implications for how materials flowing from rivers to the ocean affect carbon and nitrogen cycling.

Data availability statement

All nucleotide sequence datasets generated in this study are available in the NCBI Sequence Read Archive under the accession numbers PRJNA751272 and PRJNA751271 for the amplicon sequences of Archaea and Bacteria, respectively, and PRJNA751267 for the metagenomic sequences. Other data are available from corresponding author upon request.

References

- Andersson, A., and others. 2015. Projected future climate change and Baltic Sea ecosystem management. *Ambio* **44**: S345–S356. doi:10.1007/s13280-015-0654-8
- Azam, F., and F. Malfatti. 2007. Microbial structuring of marine ecosystems. *Nat. Rev. Microbiol.* **5**: 782. doi:10.1038/nrmicro1747
- Azetsu-Scott, K., and U. Passow. 2004. Ascending marine particles: Significance of transparent exopolymer particles (TEP) in the upper ocean. *Limnol. Oceanogr.* **49**: 741–748. doi:10.4319/lo.2004.49.3.0741
- Bao, R., M. Zhao, A. McNichol, Y. Wu, X. Guo, N. Haghypour, and T. I. Eglinton. 2019. On the origin of aged sedimentary organic matter along a river-shelf-deep ocean transect. *J. Geophys. Res. Biogeosci.* **124**: 2582–2594. doi:10.1029/2019JG005107
- Bayer, B., J. Vojvoda, T. Reinthaler, C. Reyes, M. Pinto, and G. J. Herndl. 2019a. *Nitrosopumilus adriaticus* sp. nov. and *Nitrosopumilus piranensis* sp. nov., two ammonia-oxidizing archaea from the Adriatic Sea and members of the class Nitrososphaeria. *Int. J. Syst. Evol. Microbiol.* **69**: 1892–1902. doi:10.1099/ijsem.0.003360
- Bayer, B., R. L. Hansman, M. J. Bittner, B. E. Noriega-Ortega, J. Niggemann, T. Dittmar, and G. J. Herndl. 2019b. Ammonia-oxidizing archaea release a suite of organic compounds potentially fueling prokaryotic heterotrophy in the ocean. *Environ. Microbiol.* **21**: 4062–4075. doi:10.1111/1462-2920.14755
- Bianchi, T. S. 2011. The role of terrestrially derived organic carbon in the coastal ocean: A changing paradigm and the priming effect. *Proc. Natl. Acad. Sci. USA* **108**: 19473–19481. doi:10.1073/pnas.1017982108
- Blattmann, T. M., Z. Liu, Y. Zhang, Y. Zhao, N. Haghypour, D. B. Montlucon, M. Plotze, and T. I. Eglinton. 2019. Mineralogical control on the fate of continentally derived organic matter in the ocean. *Science* **366**: 742. doi:10.1126/science.aax5345
- Bourgoin, L. H., and L. Tremblay. 2010. Bacterial reworking of terrigenous and marine organic matter in estuarine water columns and sediments. *Geochim. Cosmochim. Acta* **74**: 5593–5609. doi:10.1016/j.gca.2010.06.037
- Burkhardt, S., U. Riebesell, and I. Zondervan. 1999. Effects of growth rate, CO₂ concentration, and cell size on the stable carbon isotope fractionation in marine phytoplankton. *Geochim. Cosmochim. Acta* **63**: 3729–3741. doi:10.1016/S0016-7037(99)00217-3
- Canfield, D. E. 1994. Factors influencing organic-carbon preservation in marine-sediments. *Chem. Geol.* **114**: 315–329. doi:10.1016/0009-2541(94)90061-2
- Cao, L. J., Y. F. Gao, Y. J. Gong, J. C. Chen, M. Chen, A. Hoffmann, and S. J. Wei. 2019. Population analysis reveals genetic structure of an invasive agricultural thrips pest related to invasion of greenhouses and suitable climatic space. *Evol. Appl.* **12**: 1868–1880. doi:10.1111/eva.12847
- Carpenter, J. H. 1965. The Chesapeake Bay Institute technique for the Winkler dissolved oxygen method. *Limnol. Oceanogr.* **10**: 141–143. doi:10.4319/lo.1965.10.1.0141
- Casciotti, K. L. 2016. Nitrite isotopes as tracers of marine N cycle processes. *Phil. Trans. R. Soc. A.* **374**: 20150295. doi:10.1098/rsta.2015.0295
- Chapelle, F. H., and L. L. Knobel. 1985. Stable carbon isotopes of HCO₃ in the Aquia Aquifer, Maryland: Evidence for an isotopically heavy source of CO₂. *Groundwater* **23**: 592–599. doi:10.1111/j.1745-6584.1985.tb01507.x
- Cloern, J. E., E. A. Canuel, and D. Harris. 2002. Stable carbon and nitrogen isotope composition of aquatic and terrestrial plants of the San Francisco Bay estuarine system. *Limnol. Oceanogr.* **47**: 713–729. doi:10.4319/lo.2002.47.3.0713
- Çoban-Yıldız, Y., D. Fabbri, V. Baravelli, I. Vassura, A. Yılmaz, S. Tuğrul, and E. Eker-Develi. 2006. Analytical pyrolysis of suspended particulate organic matter from the Black Sea water column. *Deep Sea Res. Part II* **53**: 1856–1874. doi:10.1016/j.dsr2.2006.03.020
- Couturier, M., N. Tangthirasun, X. Ning, S. Brun, V. Gautier, C. Bennati-Granier, P. Silar, and J. G. Berrin. 2016. Plant biomass degrading ability of the coprophilic ascomycete fungus *Podospira anserina*. *Biotechnol. Adv.* **34**: 976–983. doi:10.1016/j.biotechadv.2016.05.010
- Dickson, A. G., C. L. Sabine, and J. R. Christian. 2007. Guide to best practices for ocean CO₂ measurements. PICES Special Publication 3. North Pacific Marine Science Organization.
- Engel, A., and others. 2005. Testing the direct effect of CO₂ concentration on a bloom of the coccolithophorid *Emiliania huxleyi* in mesocosm experiments. *Limnol. Oceanogr.* **50**: 493–507. doi:10.4319/lo.2005.50.2.0493
- Fernández-Gómez, B., M. Richter, M. Schüller, J. Pinhassi, S. G. Acinas, J. M. González, and C. Pedros-Alio. 2013. Ecology of marine Bacteroidetes: A comparative genomics approach. *ISME J.* **7**: 1026. doi:10.1038/ismej.2012.169
- Fry, B., and E. B. Sherr. 1989. δ¹³C measurements as indicators of carbon flow in marine and fresh-water ecosystems, p. 196–229. *In* P. W. Rundel, J. R. Ehleringer, and K. A. Nagy [eds.], *Stable isotopes in ecological research*. Springer. doi:10.1007/978-1-4612-3498-2_12
- Galeron, M. A., R. Amiraux, B. Charriere, O. Radakovitch, P. Raimbault, N. Garcia, V. Lagadec, F. Vaultier, and J. F. Rontani. 2015. Seasonal survey of the composition and degradation state of particulate organic matter in the Rhône River using lipid tracers. *Biogeosciences* **12**: 1431–1446. doi:10.5194/bg-12-1431-2015
- Goericke, R., and B. Fry. 1994. Variations of marine plankton δ¹³C with latitude, temperature, and dissolved CO₂ in the world ocean. *Glob. Biogeochem. Cycl.* **8**: 85–90. doi:10.1029/93GB03272

- Grigoryeva, N. I., E. V. Zhuravel, and A. A. Mazur. 2020. Seasonal variations of water quality in the Vostok Bay, Peter the Great Gulf, the Sea of Japan. *Water Resour.* **47**: 249–256. doi:10.1134/S0097807820020062
- Guo, L., and R. W. Macdonald. 2006. Source and transport of terrigenous organic matter in the upper Yukon River: Evidence from isotope ($\delta^{13}\text{C}$, $\Delta^{14}\text{C}$, and $\delta^{15}\text{N}$) composition of dissolved, colloidal, and particulate phases. *Glob. Biogeochem. Cycl.* **20**: GB2011. doi:10.1029/2005GB002593
- Hedges, J. I., R. G. Keil, and R. Benner. 1997. What happens to terrestrial organic matter in the ocean? *Org. Geochem.* **27**: 195–212. doi:10.1016/S0146-6380(97)00066-1
- Hopkinson, C. S., and J. J. Vallino. 2005. Efficient export of carbon to the deep ocean through dissolved organic matter. *Nature* **433**: 142–145. doi:10.1038/nature03191
- Hou, P., and others. 2021. Degradation and aging of terrestrial organic carbon within estuaries: biogeochemical and environmental implications. *Environ. Sci. Technol.* **55**: 10852–10861. doi:10.1021/acs.est.1c02742
- Huang, C., Q. Jiang, L. Yao, H. Yang, C. Lin, T. Huang, A. Zhu, and Y. Zhang. 2018. Variation pattern of particulate organic carbon and nitrogen in oceans and inland waters. *Biogeosciences* **15**: 1827–1841. doi:10.5194/bg-15-1827-2018
- Huang, R., and others. 2021. Elevated pCO_2 impedes succession of phytoplankton community from diatoms to Dinoflagellates along with increased abundance of viruses and bacteria. *Front. Mar. Sci.* **8**: 642208. doi:10.3389/fmars.2021.642208
- Jiao, N., and others. 2018. Unveiling the enigma of refractory carbon in the ocean. *Natl. Sci. Rev.* **5**: 459–463. doi:10.1093/nsr/nwy020
- Joachimski, M. M. 1997. Comparison of organic and inorganic carbon isotope patterns across the Frasnian-Famennian boundary. *Paleogeogr. Paleoclimatol. Paleocol.* **132**: 133–145. doi:10.1016/S0031-0182(97)00051-5
- Kandasamy, S., and B. N. Nath. 2016. Perspectives on the terrestrial organic matter transport and burial along the land-deep sea continuum: caveats in our understanding of biogeochemical processes and future needs. *Front. Mar. Sci.* **3**: 259. doi:10.3389/fmars.2016.00259
- Kiorboe, T., and G. A. Jackson. 2001. Marine snow, organic solute plumes, and optimal chemosensory behavior of bacteria. *Limnol. Oceanogr.* **46**: 1309–1318. doi:10.4319/lo.2001.46.6.1309
- Koenneke, M., J. S. Lipp, and K. U. Hinrichs. 2012. Carbon isotope fractionation by the marine ammonia-oxidizing archaeon *Nitrosopumilus maritimus*. *Org. Geochem.* **48**: 21–24. doi:10.1016/j.orggeochem.2012.04.007
- Labat, D., Y. Godd ris, J. L. Probst, and J. L. Guyot. 2004. Evidence for global runoff increase related to climate warming. *Adv. Water Resour.* **27**: 631–642. doi:10.1016/j.advwatres.2004.02.020
- Lamb, A. L., G. P. Wilson, and M. J. Leng. 2006. A review of coastal palaeoclimate and relative sea-level reconstructions using $\delta^{13}\text{C}$ and C/N ratios in organic material. *Earth-Sci. Rev.* **75**: 29–57. doi:10.1016/j.earscirev.2005.10.003
- Loh, A. N., J. E. Bauer, and E. R. M. Druffel. 2004. Variable ageing and storage of dissolved organic components in the open ocean. *Nature* **430**: 877–881. doi:10.1038/nature02780
- Lorantfy, B., B. Seyer, and C. Herwig. 2014. Stoichiometric and kinetic analysis of extreme halophilic Archaea on various substrates in a corrosion resistant bioreactor. *New Biotechnol.* **31**: 80–89. doi:10.1016/j.nbt.2013.08.003
- McDonald, N., E. P. Achterberg, C. A. Carlson, M. Gledhill, S. Liu, J. R. Matheson-Barker, N. B. Nelson, and R. J. Parsons. 2019. The role of heterotrophic bacteria and archaea in the transformation of lignin in the open ocean. *Front. Mar. Sci.* **6**: 743. doi:10.3389/fmars.2019.00743
- Meador, T. B., N. Schoffelen, T. G. Ferdelman, O. Rebello, A. Khachikyan, and M. Koenneke. 2020. Carbon recycling efficiency and phosphate turnover by marine nitrifying archaea. *Sci. Adv.* **6**: 1799. doi:10.1126/sciadv.aba1799
- Morling, K., J. Raeke, N. Kamjunke, T. Reemtsma, and J. Tittel. 2017. Tracing aquatic priming effect during microbial decomposition of terrestrial dissolved organic carbon in chemostat experiments. *Microb. Ecol.* **74**: 534–549. doi:10.1007/s00248-017-0976-0
- Opsahl, S., and R. Benner. 1997. Distribution and cycling of terrigenous dissolved organic matter in the ocean. *Nature* **386**: 480–482. doi:10.1038/386480a0
- Pelaez, F., M. J. Martinez, and A. T. Martinez. 1995. Screening of 68 species of basidiomycetes for enzymes involved in lignin degradation. *Mycol. Res.* **99**: 37–42. doi:10.1016/S0953-7562(09)80313-4
- Peters, K. E., R. E. Sweeney, and I. J. Kaplan. 1978. Correlation of carbon and nitrogen stable isotope ratios in sedimentary organic matter. *Limnol. Oceanogr.* **23**: 598–604. doi:10.4319/lo.1978.23.4.0598
- Peterson, B. J., and B. Fry. 1987. Stable isotopes in ecosystem studies. *Ann. Rev. Ecol. Syst.* **18**: 293–320.
- Rau, G. H., T. Takahashi, D. J. Des Marais, D. J. Repeta, and J. H. Martin. 1992. The relationship between $\delta^{13}\text{C}$ of organic matter and $[\text{CO}_2(\text{aq})]$ in ocean surface water: Data from a JGOFS site in the northeast Atlantic Ocean and a model. *Geochim. Cosmochim. Acta* **56**: 1413–1419. doi:10.1016/0016-7037(92)90073-R
- Raymond, P. A., and J. E. Bauer. 2001. Riverine export of aged terrestrial organic matter to the North Atlantic Ocean. *Nature* **409**: 497–500. doi:10.1038/35054034
- Redfield, A. C. 1934. On the proportions of organic derivatives in sea water and their relation to the composition of plankton. Univ. Press of Liverpool Liverpool.
- Redfield, A. C., B. H. Ketchum, and F. A. Richards. 1963. The influence of organisms on the composition of seawater, p. 26–77. In M. N. Hill [ed.], *The composition of seawater*:

- Comparative and descriptive oceanography. The sea, ideas and observations on progress in the study of the seas II, v. 2. Interscience Publishers.
- Riera, P., L. J. Stal, and J. Nieuwenhuize. 2000. Heavy $\delta^{15}\text{N}$ in intertidal benthic algae and invertebrates in the Scheldt Estuary (The Netherlands): Effect of river nitrogen inputs. *Estuar. Coast. Shelf Sci.* **51**: 365–372. doi:10.1006/ecss.2000.0684
- Seidel, M., and others. 2015. Molecular-level changes of dissolved organic matter along the Amazon River-to-ocean continuum. *Mar. Chem.* **177**: 218–231. doi:10.1016/j.marchem.2015.06.019
- Seitzinger, S. P., and R. W. Sanders. 1997. Contribution of dissolved organic nitrogen from rivers to estuarine eutrophication. *Mar. Ecol. Prog. Ser.* **159**: 1–12. doi:10.3354/meps159001
- Shannon, P., and others. 2003. Cytoscape: A software environment for integrated models of biomolecular interaction networks. *Genome Res.* **13**: 2498–2504. doi:10.1101/gr.1239303
- Sigman, D. M., K. Karsh, and K. L. Casciotti. 2009. Ocean process tracers: Nitrogen isotopes in the ocean, p. 4138–4153. *In* J. Steele, K. Turekian, and S. Thorpe [eds.], *Encyclopedia of ocean sciences*. Academic Press. doi:10.1016/B978-012374473-9.00632-9
- Sugimoto, R., A. Kasai, S. Yamao, T. Fujiwara, and T. Kimura. 2006. Short-term variation in behavior of allochthonous particulate organic matter accompanying changes of river discharge in Ise Bay, Japan. *Estuar. Coast. Shelf Sci.* **66**: 267–279. doi:10.1016/j.ecss.2005.08.014
- Thomas, H., V. Ittekkot, C. Osterroht, and B. Schneider. 1999. Preferential recycling of nutrients—The ocean's way to increase new production and to pass nutrient limitation? *Limnol. Oceanogr.* **44**: 1999–2004. doi:10.4319/lo.1999.44.8.1999
- Thornton, S. F., and J. McManus. 1994. Application of organic carbon and nitrogen stable isotope and C/N ratios as source indicators of organic matter provenance in estuarine systems: evidence from the Tay Estuary, Scotland. *Estuar. Coast. Shelf Sci.* **38**: 219–233. doi:10.1006/ecss.1994.1015
- Turner, A., and G. E. Millward. 2002. Suspended particles: Their role in estuarine biogeochemical cycles. *Estuar. Coast. Shelf Sci.* **55**: 857–883. doi:10.1006/ecss.2002.1033
- Wakeham, S. G., and E. A. Canuel. 2006. Degradation and preservation of organic matter in marine sediments, p. 295–321. *In* J. K. Volkman [ed.], *The handbook of environmental chemistry*. Springer. doi:10.1007/698_2_009
- Werth, M., and Y. Kuzyakov. 2010. ^{13}C fractionation at the root–microorganisms–soil interface: A review and outlook for partitioning studies. *Soil Biol. Biochem.* **42**: 1372–1384. doi:10.1016/j.soilbio.2010.04.009
- Wu, Y., T. Dittmar, K. U. Ludwigowski, G. Kattner, J. Zhang, Z. Y. Zhu, and B. P. Koch. 2007. Tracing suspended organic nitrogen from the Yangtze River catchment into the East China Sea. *Mar. Chem.* **107**: 367–377. doi:10.1016/j.marchem.2007.01.022
- Xavier, M., K. W. Peter, and P. R. Jennifer. 2013. Taxon-specific C/N relative use efficiency for amino acids in an estuarine community. *FEMS Microbiol. Ecol.* **83**: 402–412. doi:10.1111/j.1574-6941.12000.x
- Zhang, S., C. Liang, and W. Xian. 2020. Spatial and temporal distributions of terrestrial and marine organic matter in the surface sediments of the Yangtze River estuary. *Cont. Shelf Res.* **203**: 104158. doi:10.1016/j.csr.2020.104158
- Zhang, Y., W. Xiao, and N. Jiao. 2016. Linking biochemical properties of particles to particle-attached and free-living bacterial community structure along the particle density gradient from freshwater to open ocean. *J. Geophys. Res. Biogeosci.* **121**: 2261–2274. doi:10.1002/2016JG003390

Acknowledgments

The authors sincerely thank all members of the Aquatron team for their assistance with the experiment, especially Prof. Hugh Macintyre for his assistance with data analyses, Elizabeth Kerrigan for her assistance with nutrient measurements, Claire Normandeau for her technical assistance in using the laboratory's equipment, and Steve Fowler for his assistance with sample transportation. We also thank Drs. Douglas Wallace, Julie Laroche, Paul Hill, Rui Zhang, Shuh-ji Kao, Zihao Zhao, Lei Hou, Jinyu Yang, Tiantian Tang, and Xianhui Wan for their valuable discussions as well as John Batt, Jia Sun and Jiezheng Xie for their help with sampling. The authors also thank Steve O'Shea, PhD, from Edanz (<https://www.edanz.com/ac>), for editing a draft of this manuscript. This work was funded by the National Key Research and Development Programs (2020YFA0608300), NSFC projects (42125603, 92051114, 91751207, 42188102, 42141003, and 42230412), and Fundamental Research Funds for the Central Universities (20720200070). This study is a contribution to the international IMBeR project. This is OUC-CAMS contribution #5.

Conflict of Interest

None declared.

Submitted 23 September 2021

Revised 03 April 2022

Accepted 18 October 2022

Associate editor: Anja Engel